Design Principles for Multicuhannel Fringing Electric Field Sensors

Xiaobei B. Li, Sam D. Larson, Alexei S. Zyuzin, and Alexander V. Mamishev, *Member, IEEE*

***Abstract*—This paper presents general rules and principles for designing multichannel fringing electric field (FEF) sensors. A detailed analysis on how the design parameters, especially sensor geometry, affect the performance of FEF sensors is provided. Tradeoffs among different design objectives are explained, and qualitative design rules for balancing these tradeoffs are presented. The rules are illustrated with the design examples of two concentric FEF sensors. The effects of shielding electrode width and substrate thickness on sensor performance were evaluated through finite element simulations. In addition, the performance of the two sensors was compared based on the numerical calculations of penetration depth and signal strength. The comparison proves that the addition of shielding electrodes can improve the penetration depth of FEF sensors.**

***Index Terms*—Concentric sensor, dielectrometry, fringing electric field (FEF), imaging.**

I. Introduction

MULTICHANNEL fringing electric field (FEF) sensors are widely used to measure material properties as functions of position and time [1]–[3]. The design process of FEF sensors and sensor arrays relies on a good understanding of the fundamental principles and design tradeoffs. The purpose of this paper is to highlight the critical aspects of sensor design and to illustrate the described principles with numerical simulations and experimental results. For imaging applications, the major goal of sensor design is to achieve the optimum balance of measurement sensitivity, signal strength, imaging resolution, and measurement speed. The finite area of sensor head makes it impossible to achieve all design goals simultaneously. The task, therefore, is to consider the tradeoffs and determine the optimal combination of design variables for a given application. Design variables include the geometry of electrodes and substrate, the choice of materials for electrodes and substrate, the number of electrodes, and the arrangement of guard electrodes. The optimization process can rely on either numerical simulations [4] or analytical methods [5].

Manuscript received December 13, 2004, revised on May 13, 2005. This work was supported in part by the Center for Process Analytical Chemistry (University of Washington), in part by the Air Force Office of Scientific Research (AFOSR) under Grant F49620-02-1-0370, and in part by the National Science Foundation under Grant ECS-9523128. Undergraduate research was funded by the University of Washington EEIC scholarship and Mary Gates Scholarship. The associate editor coordinating the review of this paper and approving it for publication was Dr. Andre Bossche.

X. Li, S. D. Larson, and A. V. Mamishev are with the Department of Electrical Engineering, University of Washington, Seattle, WA 98195 USA (e-mail: shellyli@u.washington.edu; sam@ee.washington.edu; mamishev@ee.washington.edu).

A. S. Zyuzin is with the dTEC Systems LLC, Seattle, WA 98119 USA (e-mail: aszyuzin@dtecsystems.us).

Digital Object Identifier 10.1109/JSEN.2006.870161

Finite-element (FE) methods are used extensively for sensor modeling [6], optimization [7], and performance evaluation [8], especially for structures that are difficult to model analytically. The quality of the results from FE methods depends on model definition as well as mesh generation and refinement. When the right model and mesh are chosen, FE simulations can generate results with high accuracy.

It is often difficult to construct an analytical model for a three-dimensional (3-D) electrical sensor. Analytical models based on conformal mapping were constructed for interdigital structures in [9], [10]. Such a model was developed to evaluate the effects of design parameters such as finger width, substrate thickness, and metallization ratio for thin-film interdigital FEF sensors [10]. The model generated solutions that match closely with experimental data and FEM simulation results. In geometries where one of the three dimensions can be considered infinite compared with the other two, a two-dimensional model approximation can be used [11]. The effect of electric-field-bending on the linearity of a capacitive position sensor was studied based on an analytical model [12]. A similar model was constructed for an interdigital FEF sensor designed to detect the presence of water on a glass surface [13]. Based on analytical calculations, authors of [13] investigated the effect that electrode width and the width of the gap between the electrodes have on sensor output. The validity of the analytical model was proven by matching results from finite-difference (FD) simulations. Both the analytical calculation and FD simulation results showed a tradeoff between measurement sensitivity and signal strength. The paper did not address, however, the penetration depth of the sensor and how it is affected by sensor geometry. Penetration depth is an important parameter in applications where bulk measurements (as oppose to surface measurement) of the medium under test are required.

Among all of the design variables, electrode geometry is the major determining factor for sensor performance. Therefore, the choice of sensor geometry is critical to meeting the requirements of an application. Sensors of various geometries were designed previously for profiling and imaging applications. For example, a multisegment interdigital FEF sensor was used for multiphase interface detection [14]; a multisegment cylindrical sensor was used to image continuous flows of materials inside a pipeline [15]; a helical wound electrode sensor and a concave electrode sensor were developed for void fraction measurements [16]. For applications where the sample can only be accessed from one side, FEF sensors can be used. Such applications include, among others, online measurement of moisture content in food products [17], pharmaceutical products [18], and paper pulp [19], as well as cure state monitoring in the resin transfer molding process [20], [21].

Aside from sensor geometry, sensor output also depends on the sample of interest. The optimal design, therefore, is appli-

cation dependent. The current paper focuses on the qualitative effect of design parameters on sensor performance for samples with low permittivity (< 10) and low conductivity. Design of capacitance tomography sensors for media with high dielectric permittivity is investigated in [14]. The sensor was used to measure the fluid flowing in the pipe through an insulating wall. Simulation was conducted to determine the effect of wall thickness on sensor output. Although the simulation results apply only to tomography sensors of similar geometry, [14] provides insights on how the permittivity of the medium under test affects the performance of capacitive sensors in general.

The performance of FEF sensors is typically evaluated based on their penetration depth, signal strength, measurement sensitivity, and linearity. All of these factors depend on sensor geometry. The effect of electrode geometry on the performance of interdigital FEF sensors was analyzed in [22], but not in the context of imaging applications. This paper provides generalized design principles for multichannel FEF sensors with a focus on imaging applications. Most of the principles and results presented here can be applied to designing multichannel imaging sensors of other types, as well.

The first part of this paper focuses on the qualitative effect that design variables have on sensor performance. The second part of the paper illustrates the method of simulation-based design optimization through the example of two multichannel concentric sensors. The qualitative analysis from the first part provides intuitive design guidelines for the optimization process shown in the second part of the paper.

II. Figures of Merit

Penetration depth, measurement sensitivity, dynamic range, signal strength, and noise tolerance are the figures of merit usually used to evaluate the performance of multichannel FEF sensors. For imaging applications, imaging resolution and speed are also considered. All these figures of merit are analyzed in detail in this section.

A. Penetration Depth

Penetration depth is a measure of how quickly the electric field intensity decreases as the distance from the plane of sensor electrodes increases. There is no strict definition of penetration depth for FEF sensors. One way to evaluate the effective penetration depth is to position a sample above the sensor head, move it away from the sensor surface, and measure the terminal capacitance at each position. Penetration depth $\gamma_{3\%}$ corresponds to the position z where the difference between the capacitance at that position $C(z = \gamma_{3\%})$ and the asymptotic capacitance $C(z = \infty)$ equals to 3% of the difference between the highest and the lowest values of the terminal impedance [23]. This method is illustrated in (1) and Fig. 1, where $C(z = 0)$ represents the sensor terminal capacitance when the sensor is in direct contact with the sample

$$\frac{C(z = \gamma_{3\%}) - C(z = \infty)}{C(z = 0) - C(z = \infty)} \times 100\% = 3\%. \tag{1}$$

For an interdigital sensor with a 50% metallization ratio (the ratio of the area of the electrodes to the total area of the sensor surface), penetration depth $\gamma_{3\%}$ is roughly one third of its spatial wavelength λ [24]. Spatial wavelength is defined here as the distance between the centerlines of neighboring electrodes of the same type (e.g., driving or sensing electrodes).

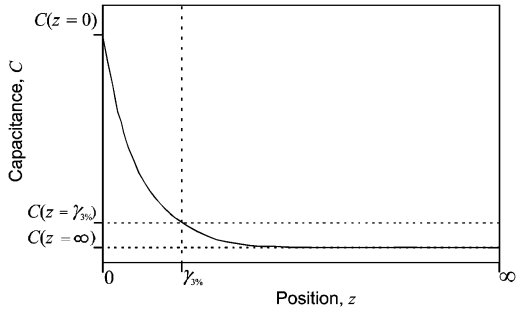

Fig. 1. Evaluation of the effective penetration depth $\gamma_{3\%}$ of an FEF sensor.

B. Measurement Sensitivity

Measurement sensitivity is defined as the ratio between the change in sensor output and the change in the measured physical parameter of the sample. Because the electric field of FEF sensors is nonuniform, their measurement sensitivity is position-dependent. As illustrated in Fig. 1, sensitivity decreases exponentially with increasing distance from the plane of electrodes.

Measurement sensitivity also depends on the area of electrodes. For a fixed spatial wavelength, a greater electrode area means higher measurement sensitivity to changes in the sample under test. In the case of multichannel sensors, however, increasing the electrode area will decrease the amount of measurement channels, if the spatial wavelength for each channel is fixed.

C. Signal Strength

FEF sensors are generally made of metal strips and the capacitance between the adjacent two strips is relatively small. This leads to low signal strength. To increase signal strength, sensors with interdigitated periodical structures can be built. Signal strength is improved here through adding more "fingers" to a sensor.

The signal strength of an FEF sensor changes exponentially with its distance to the sample. For capacitive measurements, if the dielectric permittivity of the sample is higher than that of the medium, the signal strength decays with the increasing distance to the sample. If the sensor is immersed in a medium that has finite conductivity, its signal strength can either increase or decrease depending on the dielectric properties of the medium and the sample.

D. Noise Tolerance

Guard electrodes are usually used to shield sensing electrodes from noise. They can take the form of a guard ring surrounding the active sensor electrodes (driving and sensing electrodes), the guard plane beneath the sensor substrate, or a 3-D shield around the sensing area. They need to be positioned properly for optimal sensor performance. They should also be carefully connected to avoid stray capacitances and ground loops. The driven-guard technique, where the guard electrodes are kept at the same

voltage potential as the sensing electrodes, is used to remove or reduce any stray capacitances from the guard electrodes [25].

E. Imaging Resolution

A straightforward approach to produce an image of a physical parameter of a sample is to let each measurement channel of the sensor correspond to one pixel in the image. The method has the limitation that the number of channels has to be the same as the number of desired pixels. To generate an image with high resolution, a large number of measurement channels is required, which is often difficult to implement. Tomography imaging, on the other hand, reconstructs images by interpolating measurements from different channels, and the number of pixels from such interpolation can be much greater than the number of measurement channels. However, in tomography, it is still desirable to have as many measurement channels as possible, because the degree of ill posedness in image reconstruction can be reduced by increasing the ratio of the number of independent measurements to the number of output pixels [26].

For a sensor of a fixed size, increasing the number of electrodes decreases the area of each electrode, resulting in a reduced measurement sensitivity and signal strength. If the sensor output gets close to the minimum level measurable by the interface circuit, the resulting measurement will lose accuracy. The maximum number of electrodes is, therefore, limited by the measurement resolution and the noise floor of the interface circuit.

III. Major Design Concerns

A. Surface Contact Quality

FEF sensors are highly sensitive to the composition of the volume in the immediate vicinity of the electrodes. The smaller the spatial wavelength of the sensor, the more pronounced is this effect. For applications involving contact measurements of solid samples, surface contact quality between the sample and the sensor is a major source of uncertainty. Air gaps between the sample and the electrode act as a series capacitance with the impedance of the sample and lead to inaccurate estimate of sample impedances. This air capacitance is difficult to determine because its value depends on the surface roughness of the sample and the electrodes.

To improve sensor-sample contact quality, silver paint can be applied directly to the specimen to form electrodes. Another option for improving the contact quality is the liquid immersion technique, in which the sensor and the sample are immersed in a liquid that has dielectric properties similar to that of the solid sample under test [27]. In clinical tomography applications, saline gels are applied to patients' skin to improve contact with electrodes [28].

B. Sensor Substrate and the Geometry of the Back Plane

The distance between the backplane and the driving electrode depends on the substrate thickness of the sensor. When the backplane is close to the driving electrodes, it affects the field distribution pattern, thus influencing the penetration depth and signal strength. Proper positioning and geometry design of the backplane are critical for optimizing sensor performance. The effect of substrate thickness on sensor output characteristics is illustrated with the example of two concentric FEF sensors in Section V.

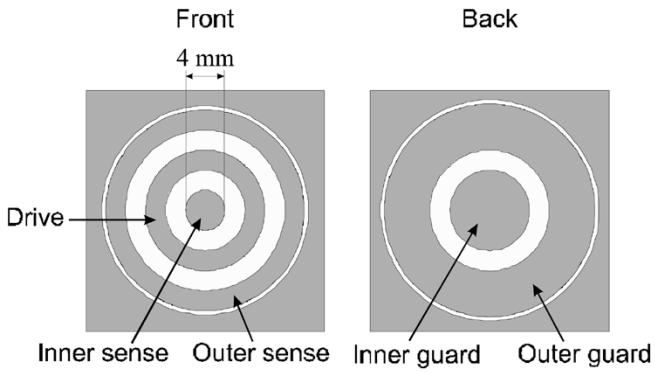

Fig. 2. Top-down view of a concentric fringing electric field sensor head. The figures were drawn to scale. The center electrode is 4 mm in diameter, as marked.

C. Crosstalk Between Different Measurement Channels

In general, the closer are individual sensing cells the stronger is the crosstalk between the corresponding channels. It is, therefore, desirable to position the sensing cells as far apart as possible. Crosstalk can also be reduced by inserting shielding electrodes between neighboring sensing cells. Both of these methods, however, reduce the total surface area of active electrodes, which, in turn, reduces measurement sensitivity and signal strength.

IV. Examples of FEF Sensor Designs

Two concentric FEF sensor designs are presented here to illustrate the qualitative design principles described in the previous sections. Fig. 2 shows a concentric sensor designed for measuring moisture content in dough [17]. The rationale for using this type of sensors in food manufacturing is available in [17]. The electrodes (black in the figure) were patterned on an insulating substrate (white in the figure). The sensor is configured as a two-channel FEF sensor, where the middle ring is used as the driving electrode and the other two electrodes are used as the sensing electrodes. Each sensing electrode needs individual guarding electrodes (the electrodes beneath the substrate) if the open voltage measurement scheme is to be used. The readers who need understanding of different measurement schemes used for this type of sensors are referred to [29].

The sensor has a spatial wavelength of 8 mm, which corresponds to a penetration depth of about 2.5 mm, a value insufficient for measuring a broad variety of food products. To increase the penetration depth, shielding electrodes are added between the driving and the sensing electrodes and are kept at the same voltage as their neighboring sensing electrode. The improved design is shown in Fig. 3. Fig. 4 illustrates the effect of the added shielding electrodes on the penetration depth of the sensor. Without the shielding electrodes, the backplane draws electric field down toward itself. The shielding electrodes counteract this effect by pushing the electric field lines upward, which effectively increases the penetration depth of the sensor. The simulation results were generated with the FEMLAB software package.

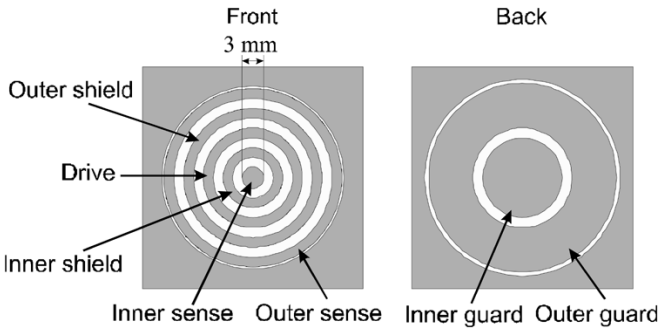

Fig. 3. Top-down view of a concentric fringing field sensor head with additional shielding electrodes between the driving and the sensing electrodes. The figures were drawn to scale. The center electrode is 3 mm in diameter.

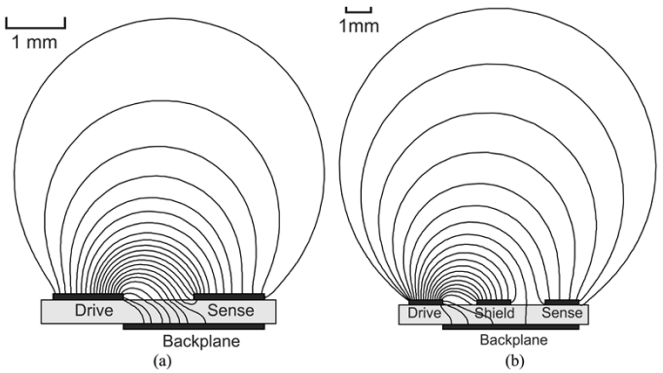

Fig. 4. Simulated electric field line distribution illustrating the effect of the additional shielding electrode. (a) The electric field line distribution of the design in Fig. 2. (b) The electric field line distribution of the design in Fig. 3.

A. FE Analysis

To compare the performance of the two designs, the software package Maxwell 2D by Ansoft Corp. was used for FE simulations. Fig. 5(a) and (b) shows the layout of the simulation spaces. These spaces were defined in radial coordinates, with the origin placed at the lower left corner of the simulation space. The driving electrode is set to 6 V and all other electrodes (including the backplane) are set to 0 V, a Dirichlet boundary condition in nature. A test sample with relative dielectric permittivity $\varepsilon_r = 5.0$ and conductivity $\sigma = 0$ is positioned above the sensor. FR4 epoxy with relative dielectric permittivity $\varepsilon_r = 4.4$ and conductivity $\sigma = 0$ is used for the substrate of the sensor. The boundary of the simulation space is set as a "charge balloon." A charge balloon models an electrically insulated system, where the charge at infinity balances the charge within the simulation space forcing the net charge to be zero. The convergence criterion for total energy error is set to be within 1%. In the simulation, the distance of the sample to the plane of sensor electrodes is varied from 15 to 0 mm. The signal strength for each sensor is evaluated based on its absolute terminal capacitance, while the penetration depth $\gamma_{3\%}$ is evaluated based on normalized terminal capacitance calculations.

B. Effect of the Shielding Electrode

Figs. 6 and 7 show, respectively, the absolute and normalized terminal capacitance values obtained from the simulation. "Sensor 1" refers to the design without the shielding electrodes in Fig. 5(a) and "Sensor 2" refers to the design with the shielding electrodes in Fig. 5(b). For both designs, the outer channel has greater signal strength than its respective inner

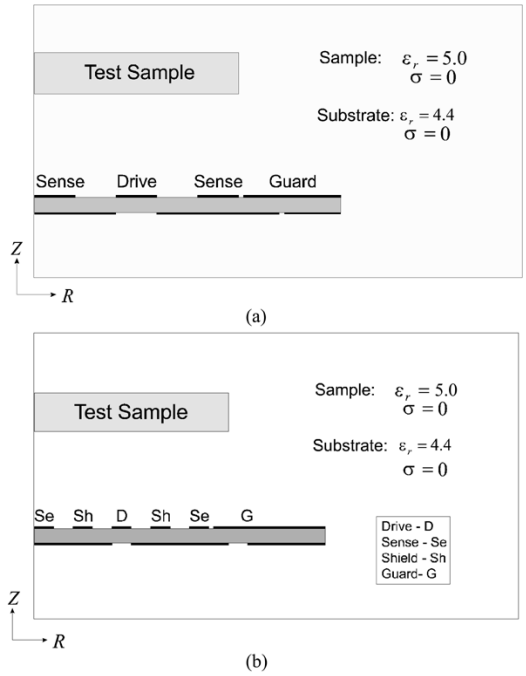

Fig. 5. Layout of a test sample positioned above (a) the shielded and (b) the shielded concentric FEF sensor in the FE simulation.

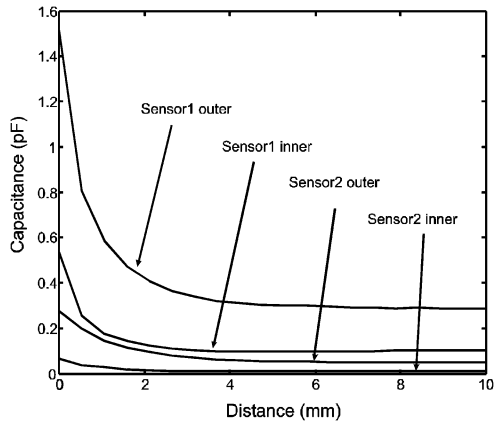

Fig. 6. Absolute capacitance value from both sensor designs in the FE simulation.

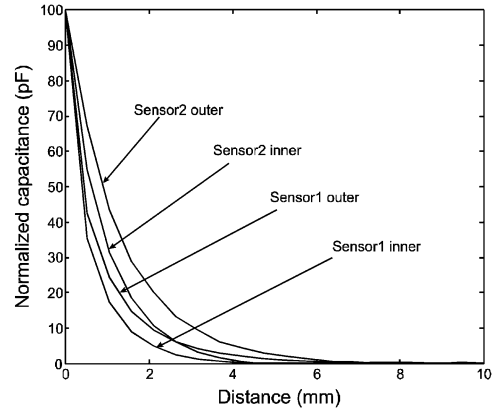

Fig. 7. Normalized capacitance value from both sensor designs in the FE simulation.

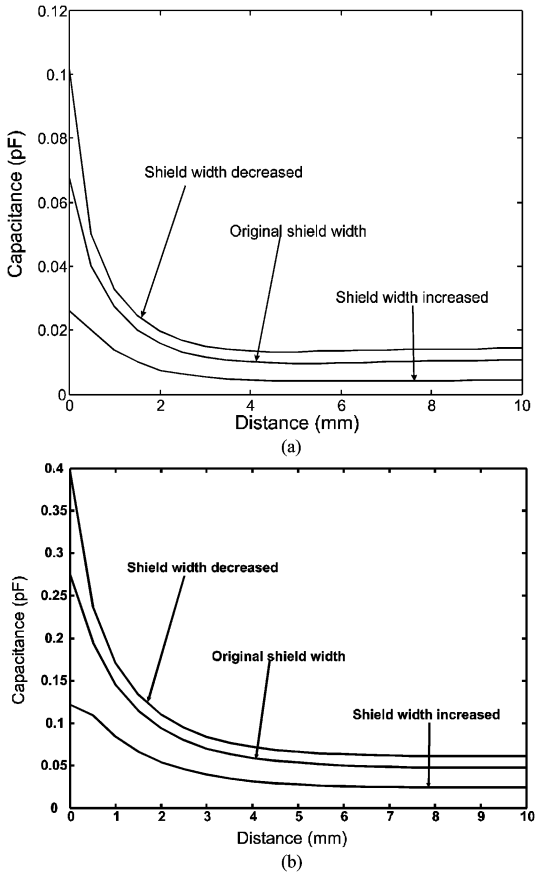

Fig. 8. Effect of change in shielding electrode width on the signal strength of the (a) inner sensing channel and (b) outer sensing channel of the shielded sensor. The results show that the sensor signal strength decreases with increasing width of the shielding electrodes.

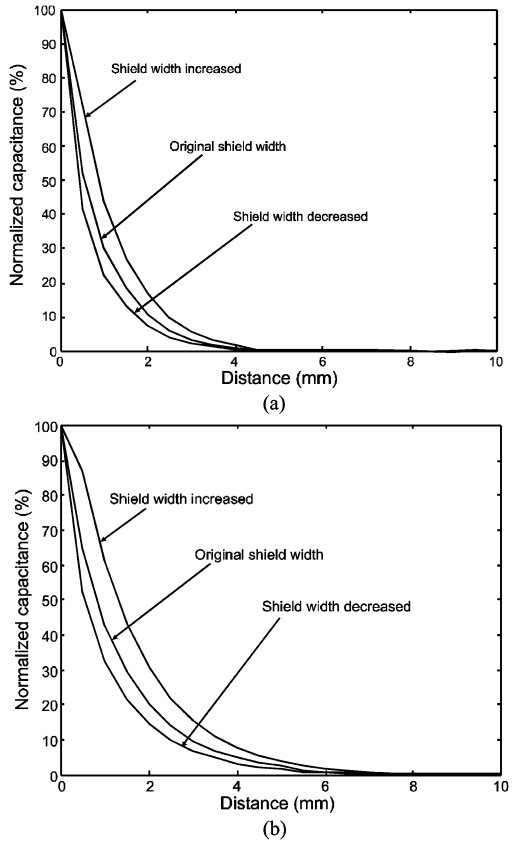

Fig. 9. Effect of change in shielding electrode width on the penetration depths of the (a) inner sensing channel and (b) outer sensing channel of the shielded sensor. The results show that the sensor penetration depth increases with increasing width of the shielding electrodes.

channel, a difference caused by the larger sensing area of the outer channel. When the performance of the two designs is compared, the second design does provide greater penetration depth than the first one. This gain in penetration depth, however, is obtained at the cost of reduced signal strength, as shown in Fig. 6.

C. Effect of the Width of the Shielding Electrode

The width of the shielding electrodes is varied in the second design to evaluate its effect on sensor output characteristics. Figs. 8 and 9 show, respectively, the absolute and normalized capacitance value of the shielded sensor when the width of the shielding electrode is varied.

The same trend exists for the capacitance value from both the inner and the outer sensing channel: When the width of the shielding electrodes increases, the sensor signal strength drops and its penetration depth increases. The trend can be explained with the help of Fig. 4(a). Wider shielding electrode diverts electric field energy away from the sensing electrodes, thus decreasing the signal strength; on the other hand, the field lines are pushed further up due to the increased surface area of the shielding electrodes, which increases the penetration depth.

D. Effect of Substrate Thickness

As illustrated in Fig. 4, the sensor backplane draws electric field energy away from the sensing electrodes. The closer the backplane is to the driving electrode, the more energy is drawn away. The distance between the driving electrode and the backplane is determined by the thickness of the substrate. The effect of substrate thickness variation is, therefore, important.

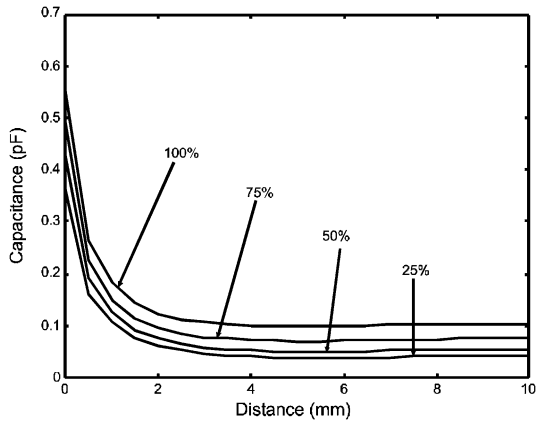

Fig. 10. Absolute capacitance value of the inner channel of the unshielded sensor with different substrate thickness.

The thickness of the sensor substrate is varied from 100% to 25% of its original value in a series of FE simulations. Fig. 10 shows the absolute capacitance value from the inner channel of the unshielded design. The results show that the closer the backplane is to the driving electrode, the weaker is the signal strength. This same trend exists for the capacitance value from both channels of the two designs.

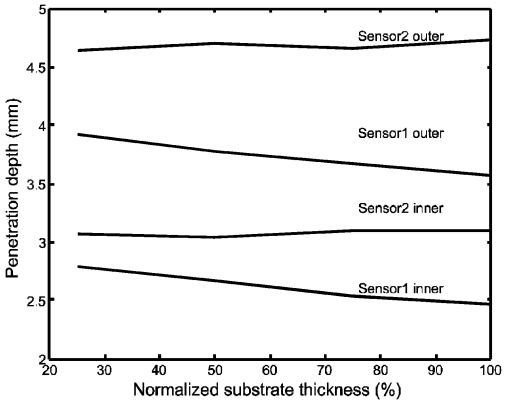

Fig. 11. Effect of change in substrate thickness on sensor penetration depth.

In addition to the signal strength, penetration depth is also affected by change in substrate thickness. The results are shown in Fig. 11. The penetration depth of the first design decreases with increasing substrate thickness. This can again be explained with the illustration in Fig. 4. The farther away the backplane is positioned from the driving electrode, the further down the electric field lines are drawn away from the top electrodes, resulting in a decreased penetration depth. Penetration depth for the second design is relatively stable against the variation in substrate thickness because of the shielding electrodes. There again exits a tradeoff between the penetration depth and signal strength: For greater signal strength, a thicker substrate is desirable, but this decreases the penetration depth of the sensor.

The sensitivity of the sensor terminal measurement to the changes in the substrate thickness depends on the ratio of the dielectric permittivity of the sample and that of the sensor substrate. For samples with a much higher dielectric permittivity than the permittivity of the substrate, variation in substrate thickness will not affect the sensor performance as much.

V. Limitations of Simulation Results

It is worth noting that the optimization results presented in this paper are application-dependent. The optimal sensor geometry changes with respect to different samples. In the simulations of this paper, samples with low permittivity (< 10) and close to zero conductivity were used. Such samples are representative for a wide range of ceramics and plastics [30]. Design of sensors specialized for high permittivity dielectrics $(10 < \varepsilon_r < 80)$ were discussed in [15]. For highly conductive samples, resistance, instead of capacitance, is measured to estimate sample concentration or distribution within the sensing zone. In cases where the sample has complex permittivity and displays frequency-dependent behavior, both the real part and the imaginary part of the complex impedance have to be measured.

The multichannel impedance sensors presented in this paper are designed for industrial process imaging applications. Electrical tomography systems typically operate in the sub-megahertz range. Therefore, the electrostatic model used in the FE simulations is adequate. For sensors used in broad-band spectroscopic systems, AC simulations are necessary. Such systems are usually used for lab-based determination of material properties of samples with complex permittivity.

VI. Conclusion

This paper presents the design principles for multichannel FEF sensors, with a special focus on the analysis of figures of merit and the major tradeoffs caused by various design constraints. The effect of design variables, especially sensor geometry, on sensor performance is analyzed. These qualitative guidelines help to understand the logic behind the simulation-based design procedures used for the two concentric FEF sensors. The performance of the two sensors is compared. The shielding electrodes added in the second design were shown to increase the penetration depth of the sensor. In addition, the effects of substrate thickness and shielding electrode width were evaluated. The simulation results demonstrated the effects of sensor geometry on its performance and provided insights into the design process of FEF sensors.

Acknowledgment

The authors would like to thank undergraduate student C. Kato for her contribution to the FE simulations.

References

[1] Y. K. Sheiretov and M. Zahn, "Dielectrometry measurements of moisture dynamics in oil-impregnated pressboard," *IEEE Trans. Dielectr. Electr. Insul.*, vol. 2, no. , pp. 329–351, Jun. 1995.

[2] N. F. Sheppard Jr, S. L. Garverick, D. R. Day, and S. D. Senturia, "Microdielectrometry: A New method for in situ cure monitoring," in *Proc. 26th SAMPE Symp.*, Los Angeles, CA, 1981, pp. 65–76.

[3] V. Shtrauss, A. Kalpinsh, U. Lomanovskis, and J. Rotbahs, "Tomographic imaging by electrical methods," *Latvian J. Phys. Tech. Sci.*, no. 3, pp. 23–47, 1995.

[4] S. H. Khan and F. Abdullah, "Finite-Element modeling of multielectrode capacitive systems for flow imaging," *Proc. Inst. Elect. Eng. G, Circuits Devices Syst.*, vol. 140, no. 3, pp. 216–222, 1993.

[5] X. J. Li, G. deJong, and G. C. M. Meijer, "The application of the capacitor's physics to optimize capacitive angular-position sensors," *IEEE Trans. Instrum. Meas.*, vol. 46, no. 1, pp. 8–14, Feb. 1997.

[6] M. H. W. Bonse, C. Mul, and J. W. Spronck, "Finite-Element modeling as a tool for designing capacitive position sensors," *Sens. Actuators A*, vol. 46, no. 1–3, pp. 266–269, 1995.

[7] S. H. Khan and F. Abdullah, "Finite-Element modeling of multielectrode capacitive systems for flow imaging," *Proc. Inst. Elect. Eng. G, Circuits Devices Syst.*, vol. 140, no. 3, pp. 216–222, 1993.

[8] S. H. Khan, L. Finkelstein, and F. Abdullah, "Investigation of the effects of design parameters on output characteristics of capacitive angular displacement sensors by finite element field modeling," *IEEE Trans. Magn.*, vol. 33, no. 2, pp. 2081–2084, Mar. 1997.

[9] S. S. Gevorgian, T. Martinsson, P. L. J. Linner, and E. L. Kollberg, "CAD models for multilayered substrate interdigital capacitors," *IEEE Trans. Microw. Theory Tech.*, vol. 44, no. 6, pp. 896–904, Jun. 1996.

[10] R. Igreja and C. J. Dias, "Analytical evaluation of the interdigital electrodes capacitance for a multi-layered structure," *Sens. Actuators A*, vol. 112, no. 2–3, pp. 291–301, 2004.

[11] W. C. Heerens, "Application of capacitance techniques in sensor design," *J. Phys. E, Sci. Instrum.*, vol. 19, no. 11, pp. 897–906, 1986.

[12] X. J. Li, G. de Jong, and G. C. M. Meijer, "The influence of electric-field bending on the nonlinearity of capacitive sensors," *IEEE Trans. Instrum. Meas.*, vol. 49, no. 2, pp. 256–259, Apr. 2000.

[13] N. Boules and T. W. Nehl, "Design optimization of glass-embedded capacitive-type water sensors," *IEEE Trans. Ind. Appl.*, vol. 24, no. 3, pp. 402–410, May/Jun. 1988.

[14] H. X. Wang, W. L. Yin, W. Q. Yang, and M. S. Beck, "Optimum design of segmented capacitance sensing array for multi-phase interface measurement," *Meas. Sci. Technol.*, vol. 7, no. 1, pp. 79–86, 1996.

[15] A. J. Jaworski and G. T. Bolton, "The design of an electrical capacitance tomography sensor for use with media of high dielectric permittivity," *Meas. Sci. Technol.*, vol. 11, no. 6, pp. 743–757, 2000.

[16] K. J. Elkow and K. S. Rezkallah, "Void fraction measurements in Gas-Liquid flows under 1-g and Mu-g conditions using capacitance sensors," *Int. J. Multiphase Flow*, vol. 23, no. 5, pp. 815–829, 1997.

[17] X. Li, A. Zyuzin, and A. V. Mamishev, "Measuring moisture content in cookies using dielectric spectroscopy," presented at the IEEE Conf. Electrical Insulation and Dielectric Properties, 2003.
[18] M. Craig, "Dielectric spectroscopy as a novel analytical technique within the pharmaceutical sciences," *STP-Pharma-Pratiques*, vol. 5, no. 6, pp. 421–42, 1995.
[19] K. Sundara-Rajan, L. Byrd, and A. V. Mamishev, "Moisture content estimation in paper pulp using fringing field impedance spectroscopy," *IEEE Sensors J.*, no. 3, pp. 378–383, Jun. 2004.
[20] A. A. Ogale, M. C. Hegg, A. Mescher, A. V. Mamishev, and B. Minae, "Fill front detection using dielectric sensors in resin transfer molding processes," in *Proc. Int. Conf. Composites/Nano Engineering*, 2003, pp. 529–530.
[21] C. W. Lee, B. P. Rice, M. Buczek, and D. Mason, "Resin transfer process monitoring and control," *SAMPE J.*, vol. 34, no. 6, pp. 48–55, Nov. 1998.
[22] A. V. Mamishev, A. R. Takahashi, Y. Du, B. C. Lesieutre, and M. Zahn, "Assessment of performance of fringing electric field sensor arrays," in *Proc. IEEE Conf. Electrical Insulation and Dielectric Phenomena*, 2002, pp. 918–921.
[23] A. V. Mamishev, B. C. Lesieutre, and M. Zahn, "Optimization of multiwavelength interdigital dielectrometry instrumentation and algorithms," *IEEE Trans. Dielectr. Electr. Insul.*, no. 3, pp. 408–420, Jun. 1998.
[24] A. V. Mamishev, Y. Du, J. H. Bau, B. C. Lesieutre, and M. Zahn, "Evaluation of diffusion-driven material property profiles using three-wavelength interdigital sensor," *IEEE Trans. Dielectr. Electr. Insul.*, vol. 8, no. 5, pp. 785–798, Oct. 2001.
[25] R. Pallas-Areny and J. G. Webster, *Sensors and Signal Conditioning*, 2nd ed. New York: Wiley, 2001.
[26] G. Demoment, "Image-Reconstruction and restoration—Overview of common estimation structures and problems," *IEEE Trans. Acoust. Speech Signal Process.*, vol. 37, no. 12, pp. 2024–2036, Dec. 1989.
[27] A. V. Mamishev, "Interdigital Dielectrometry Sensor Design and Parameter Estimation Algorithms for Nondestructive Materials Evaluation," Ph.D. dissertation, Dept. Elect. Eng. Comput. Sci., Mass. Inst. Technol., Cambridge, 1999.
[28] J. G. Webster, *Electrical Impedance Tomography*, J. G. Webster, Ed. New York: Adam Hilger, 1990, pp. 21–28.
[29] A. V. Mamishev, K. Sundara-Rajan, F. Yang, Y. Q. Du, and M. Zahn, "Interdigital sensors and transducers," *Proc. IEEE*, vol. 92, no. 5, pp. 808–845, May 2004.
[30] A. von Hippel, *Dielectric Materials and Applications*. Norwood, MA: Artech House, 1995.

Xiaobei B. Li received the B.S. degree in controls theory from Northwestern Polytechnical University, Xi'an, China, in 1999, and the M.S. degree in electrical engineering from the University of Washington (UW), Seattle, in 2003. She is currently pursuing the Ph.D. degree at the Sensors, Energy, and Automation Laboratory (SEAL), Department of Electrical Engineering, UW.

Her research interests include dielectric spectroscopy sensor design, sensor signal conditioning circuit design, and image reconstruction for soft-field sensing. In January 2006, she joined the Power Thermal Pathfinding Technology Lab, Intel Corporation, Dupont, WA.

Sam D. Larson received the B.S. degree in electrical engineering from the University of Washington, Seattle, in 2004, where he is currently pursuing the M.S. degree in the Department of Electrical Engineering.

Alexei S. Zyuzin received the B.S. degree in electrical engineering from the University of Washington (UW), Seattle, in 2004.

From 2002 to 2004, he was an Undergraduate Research Assistant at the Sensors, Energy, and Automation Laboratory (SEAL), Department of Electrical Engineering, UW. Since 2003, he has been a Research Electrical Engineer with dTEC Systems LLC, Seattle. His research interests include the development of novel analytical instruments and sensor systems for chemical contamination monitoring in soil and water samples utilizing ion mobility and electric field spectroscopy techniques.

Alexander V. Mamishev (M'00) received the equivalent of the B.S. degree in electrical engineering from the Kiev Polytechnic Institute, Ukraine, in 1992, the M.S. degree in electrical engineering from Texas A&M University, College Station, in 1994, and the Ph.D. degree in electrical engineering from the Massachusetts Institute of Technology (MIT), Cambridge, with a minor in technology management from Harvard Business School, Cambridge, and the MIT Sloan School of Management, in 1999.

Currently, he is an Associate Professor, Director of Sensors, Energy, and Automation Laboratory (SEAL), and Director of Electrical Energy Industrial Consortium (EEIC) with the Department of Electrical Engineering, University of Washington, Seattle. He is the author of one book chapter, about 80 journal and conference papers, one book chapter, and one patent. His research interests include sensor design and integration, robotics, and energy technology applications. He is currently the Director of the Sensors, Energy, and Automation Laboratory (SEAL), Department of Electrical Engineering, University of Washington.

Dr. Mamishev is a recipient of the NSF CAREER Award, the IEEE Outstanding Branch Advisor Award, and the UW EE Outstanding Research Advisor Award. He serves as an Associate Editor for the IEEE TRANSACTIONS ON DIELECTRICS AND ELECTRICAL INSULATION, as well as reviewer for several journals and conferences.